ISSN 1674-1056
http://cpb.iphy.ac.cn
http://iopscience.iop.org/cpb
中国物理 B
Chinese Physics
中国物理 Chinese Physics B

Photoluminescence of SiV centers in CVD diamond particles with specific crystallographic planes

Ying-Shuang Mei(梅盈爽), Cheng-Ke Chen(陈成克), Mei-Yan Jiang(蒋梅燕), Xiao Li(李晓), Yin-Lan Ruan(阮银兰), Xiao-Jun Hu(胡晓君)

Citation: Chin. Phys. B . 2019, 28(1): 016101. **doi:** 10.1088/1674-1056/28/1/016101
Journal homepage: http://cpb.iphy.ac.cn; http://iopscience.iop.org/cpb

What follows is a list of articles you may be interested in

Increase of photoluminescence blinking frequency of 3C-SiC nanocrystals with excitation power

Zhixing Gan(甘志星), Weiping Zhou(周卫平), Ming Meng(孟明)

Chin. Phys. B . 2018, 27(12): 127804. **doi:** 10.1088/1674-1056/27/12/127804

Photodynamics of Ga_{Zn}-V_{Zn} complex defect in Ga-doped ZnO

Ai-Hua Tang(汤爱华), Zeng-Xia Mei(梅增霞), Yao-Nan Hou(侯尧楠), Xiao-Long Du(杜小龙)

Chin. Phys. B . 2018, 27(11): 117802. **doi:** 10.1088/1674-1056/27/11/117802

Recent progress on photoluminescence from plasmonic nanostructures: Phenomenon, mechanism, and application

Tingting Yin(尹婷婷), Liyong Jiang(蒋立勇), Zexiang Shen(申泽骧)

Chin. Phys. B . 2018, 27(9): 097803. **doi:** 10.1088/1674-1056/27/9/097803

Transition intensity calculation of Yb: YAG

Hong-Bo Zhang(张洪波), Qing-Li Zhang(张庆礼), Xing Wang(王星), Gui-Hua Sun(孙贵花), Xiao-Fei Wang(王小飞), De-Ming Zhang(张德明), Dun-Lu Sun(孙敦陆)

Chin. Phys. B . 2018, 27(6): 067801. **doi:** 10.1088/1674-1056/27/6/067801

Magneto-optical properties of self-assembled InAs quantum dots for quantum information processing

Jing Tang(唐静), Xiu-Lai Xu(许秀来)

Chin. Phys. B . 2018, 27(2): 027804. **doi:** 10.1088/1674-1056/27/2/027804

Photoluminescence of SiV centers in CVD diamond particles with specific crystallographic planes*

Ying-Shuang Mei(梅盈爽)[1], Cheng-Ke Chen(陈成克)[1], Mei-Yan Jiang(蒋梅燕)[1], Xiao Li(李晓)[1], Yin-Lan Ruan(阮银兰)[2], and Xiao-Jun Hu(胡晓君)[1,†]

[1] *College of Materials Science and Engineering, Zhejiang University of Technology, Hangzhou* 310014, *China*

[2] *ARC Centre of Excellence in Nanoscale Biophotonics, Institute of Photonics and Advanced Sensing, University of Adelaide, Adelaide* 5005, *Australia*

(Received 3 August 2018; revised manuscript received 17 October 2018; published online 30 December 2018)

We prepared the isolated micrometer-sized diamond particles without seeding on the substrate in hot filament chemical vapor deposition. The diamond particles with specific crystallographic planes and strong silicon-vacancy (SiV) photoluminescence (PL) have been prepared by adjusting the growth pressure. As the growth pressure increases from 2.5 to 3.5 kPa, the diamond particles transit from composite planes of {100} and {111} to only smooth {111} planes. The {111}-faceted diamond particles present better crystal quality and stronger normalized intensity of SiV PL with a narrower bandwidth of 5 nm. Raman depth profiles show that the SiV centers are more likely to be formed on the near-surface areas of the diamond particles, which have poorer crystal quality and greater lattice stress than the inner areas. Complex lattice stress environment in the near-surface areas broadens the bandwidth of SiV PL peak. These results provide a feasible method to prepare diamond particles with specific crystallographic planes and stronger SiV PL.

Keywords: diamond particle, SiV center, photoluminescence, crystallographic planes

PACS: 61.72.jn, 78.20.–e, 81.05.ug **DOI:** 10.1088/1674-1056/28/1/016101

1. Introduction

Diamonds with many excellent characteristics have great application potential in the fields of physics, chemistry, and biology.[1–3] Among them, color centers in diamond have attracted intense research interest in recent years due to the unique fluorescence characteristics and application potential in quantum physics and biology.[4,5] The silicon-vacancy (SiV) center is attractive due to its very narrow band (approximately 5 nm), 70% of its fluorescence concentrated in ZPL at 738 nm, and short luminescence lifetime (approximately 1.2 ns).[6,7] These distinguishable properties make the SiV center suitable for quantum information processing. Moreover, the near-infrared PL of the SiV center is far away from that of the cellular auto-fluorescence in the visible wavelength, which enables the SiV center ideal bio-labeling for biological and medical applications.[8]

To meet different applications as mentioned above, it is necessary to prepare micro- or nano-scale isolated diamond with applicable properties of SiV PL. Using chemical vapor deposition (CVD), Si impurities can diffuse from the silicon substrate or reaction gas source into diamond grains, forming SiV centers.[9] The SiV center has a ⟨111⟩ aligned split-vacancy structure with D_{3d} symmetry.[6,10,11] If the emitting dipole is oriented perpendicularly to the symmetry axis, the photon emission for the SiV center is predicted to be optimal. It is shown that the {111} planes made the largest contribution to the emission collected efficiency of SiV PL in microcrystalline diamond films deposited on AlN substrates.[12] This suggests that the diamond particles consisting of {111} planes may have high intensity of SiV PL. However, to the best of our knowledge, there have been no reports on the controllable preparation of SiV photoluminescent diamond particles with {111} planes.

It was found that the substrate temperature, reaction gas composition, and growth pressure during the CVD would affect the growth of diamond crystal planes.[13–16] Researchers believed that different parameters led to the interactions between surface atoms and foreign atoms, producing different surface free energies and crystal planes,[13–16] while it is very difficult to determine the surface free energy because of the complex growth environment.[15,16] In hot-filament CVD (HFCVD) systems, the growth pressure affects the formation of different crystal planes of diamond particles,[17,18] but these samples contain rough crystal faces and the SiV PL has not yet been investigated. In addition, nanodiamonds or precursors were usually used as seeds to grow isolated diamond particles,[19–22] which probably contain nitrogen to affect the SiV PL.[21,22] The initial morphology and dispersion of the seeds may affect the distribution of the deposited samples.

*Project supported by the National Natural Science Foundation of China (Grant Nos. 50972129 and 50602039), the International Science Technology Cooperation Program of China (Grant No. 2014DFR51160), the National Key Research and Development Program of China (Grant No. 2016YFE0133200), European Union's Horizon 2020 Research and Innovation Staff Exchange (RISE) Scheme (Grant No. 734578), One Belt and One Road International Cooperation Project from Key Research and Development Program of Zhejiang Province, China (Grant No. 2018C04021), and the Natural Science Foundation of Zhejiang Province, China (Grant No. LY18E020013).

†Corresponding author. E-mail: huxj@zjut.edu.cn

© 2019 Chinese Physical Society and IOP Publishing Ltd

Thus, in order to more effectively control the diamond shape and crystal quality to obtain the strong SiV photoluminescent diamond particles, we prepared diamond particles on silicon without nanodiamond seeds by adjusting the growth pressure.

The results show that with the increase of growth pressure from 2.5 to 3.5 kPa, the diamond crystal transits from composite planes of {100} and {111} to only {111} planes. The {111}-faceted diamond particles show stronger SiV PL and better crystal quality. Moreover, the Raman depth profiles show that the SiV centers are more likely to be formed on the near-surface areas of the diamond particles, which have poorer crystal quality and greater lattice stress than the inner areas. Complex lattice stress environment in the near-surface areas broadens the bandwidth of SiV PL peak. These results demonstrate a feasible way to prepare diamond particles with specific morphology and stronger SiV PL.

2. Experiments

The isolated micrometer-sized diamond particles were grown on the Si (111) wafers by the HFCVD system. The silicon substrate was not polished or coated with nanodiamond seeds and was only cleaned by ultrasonic oscillation with acetone for 10 min and deionized water for 3 min before deposition. The HFCVD parameters are: the hot filament power is 2000 W, the substrate temperature is approximately 800 ℃, the distance between the hot filament and the substrate is 10 mm, and the gas mixture composition of CH_3COCH_3:H_2 = 40 : 200 sccm. We chose the growth pressure as 1.5, 2.5, 3.5, and 4.5 kPa, respectively, to prepare the isolated diamond particles to generate different crystal planes. The deposition time was 2–8 hours.

Scanning electron microscopy (SEM, Czech Republic) was used to observe distribution and crystal morphologies of diamond particles. The room-temperature Raman and PL single-point tests were recorded in the same area of the samples by using Lab RAM HRUV80 C (λ = 514 nm) with a laser power of 2 mW and an acquisition time of 30 s and 1 s, respectively. The spot diameter of the laser is approximately 500 nm, which ensures that the target particles are not disturbed by the signals of the surrounding particles. The Raman and PL depth profiles were recorded by Renishaw inVia Reflex (λ = 532 nm) with a laser power of 2.5 mW and an acquisition time of 10 s and 0.5 s, respectively. At first, the laser was focused on the upper surface of the diamond particles, and then the focus shifted vertically through the diamond to the Si substrate with an interval of 100 nm, recording a series of data on the vertical depth of the entire diamond particles. We chose the particles with the target shape for testing, but the placement of the particles is random. This testing method results in subtle differences in several data between diamond particles in different placements, while this difference is smaller than that caused by the solid geometry of diamond particles. In this apparatus, the spot diameter of the laser is approximately 500 nm, so the Raman and PL depth profiles tests can reflect the changing trend of the crystal structure with depth in the whole particle. Especially when the size of the diamond particles reaches several micrometers, the difference between the surface and the inner region of the particles can be effectively obtained. In order to consider the average level of particle characteristics, for the samples of each growth condition, we collected data of five diamond particles, and then calculated their mean and standard deviation.

3. Results and discussion

Figure 1 shows the SEM images of samples grown under all the selected pressures for 4 h. In the case of growth pressure of 1.5 kPa, the diamond particles have a rough surface and an irregular shape with a size of approximately 4 μm. When the growth pressure increases to 2.5 kPa, the sizes of diamond particles decrease to about 2 μm and the shape becomes cubo-octahedral, which consists of smooth square {100} and triangle {111} planes. With the growth pressure increasing to 3.5 kPa, the diamond surfaces become smooth {111} planes with a small size of ∼ 1.5 μm. Further increasing the growth pressure to 4.5 kPa, only a small part of the diamonds consists of {111} planes, while irregular crystal planes occur in most of the diamonds. These results suggest that the appropriate growth pressure can adjust the crystal faces and the size of diamond particles, in which higher pressure leads to lower growth rate and smaller size.

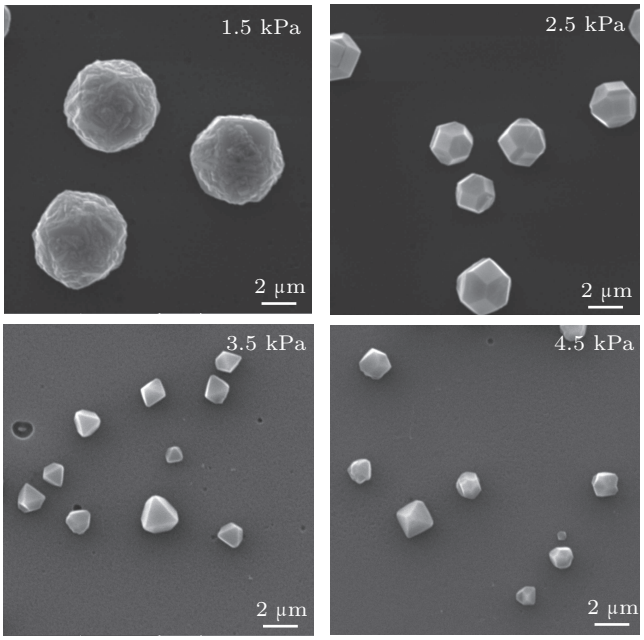


Fig. 1. SEM images of isolated diamond particles grown at the pressure of 1.5–4.5 kPa for 4 h.

Figures 2(a) and 2(b) present the typical PL spectra, their normalized intensity, and full width at half maximum

(FWHM) values of one of the diamond particles under different growth pressures, showing that all samples include the characteristic fluorescent peak of the SiV center at 738 nm. Also, there is a characteristic peak at about 552 nm, which is the diamond signal appearing in the PL spectrum, as shown in the inset of Fig. 2(a). Here the normalized intensity of the SiV peak is characterized by the intensity ratio of the SiV peak to diamond peak near 552 nm.[23] It is observed that the dependence of the SiV PL on the growth pressure is not linear. The diamond particles grown under 3.5 kPa have the strongest normalized SiV PL up to 26.9 and the smallest SiV FWHM values of 5.0 nm. These observations indicate that the diamond particles with the exposed surface of {111} planes have the most excellent SiV PL properties.

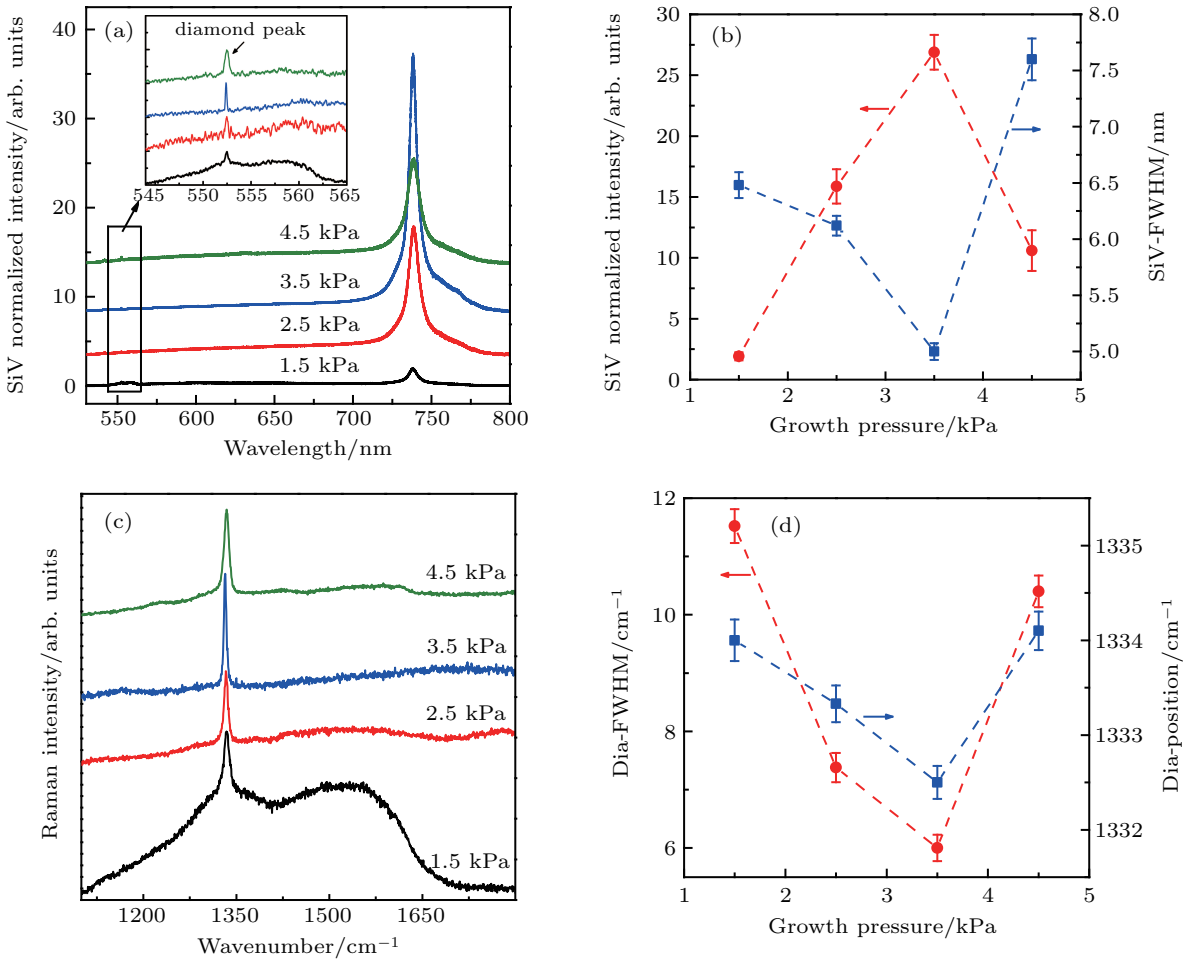


Fig. 2. (a) Typical PL spectra and (c) visible Raman spectra of samples grown at the pressure of 1.5–4.5 kPa for 4 h (one of the diamond particles for each growth pressure). (b) The normalized intensity and FWHM of SiV fluorescence peak in PL spectra and (d) the position and FWHM of the diamond peak in Raman spectra (averaged over 5 diamond particles for each growth pressure). Here the normalized intensity of SiV peak is characterized by the intensity ratio of SiV peak to diamond Raman peak near 551.8 nm in PL spectrum.

The Raman spectra shown in Fig. 2(c) display that all of the samples have an obvious peak near 1332 cm^{-1}, which is related to diamond.[19,20] In addition to 1.5 kPa, the samples grown under other pressures do not have a non-diamond carbon signal between 1400 and 1600 cm^{-1},[21,24] which could quench the emission of the color centers,[25,26] so that the diamond particles without non-diamond carbon exhibit stronger PL intensity. Figure 2(d) shows the dependence of FWHM and position of diamond peaks on the growth pressures, implying the crystalline perfection and the lattice stress, respectively.[21,23] It is observed that the diamond particles grown at 3.5 kPa have a diamond peak with the smallest FWHM value and its peak position closer to that of the ideal diamond of 1332 cm^{-1}. This indicates that the {111}-faceted diamond particles have the best crystal quality and small lattice stress among all the samples, which induces the highest PL intensity and the narrowest bandwidth in its SiV fluorescent peak.

In order to further investigate the microstructure and SiV PL performance of the diamond particles with different shapes, we fabricated a series of isolated diamond particles with a growth time of 3–8 h under the growth pressure of 2.5 and 3.5 kPa, which can produce single-crystal faceting according to the above results. Figure 3 shows their SEM images. It is observed that all of the isolated diamond particles grown under 2.5 kPa consist of triangle {111} planes and square {100}

planes. The {111} and {100} planes are both very smooth when the growth time is less than 6 h, while the {111} planes become smaller and rougher when the growth time is more than 6 h. It means that the growth rate of the [111] directions is faster than the [100] directions. In the case of 3.5 kPa, most of the isolated diamond particles show an octahedral structure consisting of triangle {111} planes. With increasing growth time, the {111} planes remain smooth, meaning that the diamond particles keep better crystal quality. Also, the size of diamond particles grown at 3.5 kPa is smaller than those grown at 2.5 kPa for the same growth time, indicating the slower growth rate in the case of 3.5 kPa.

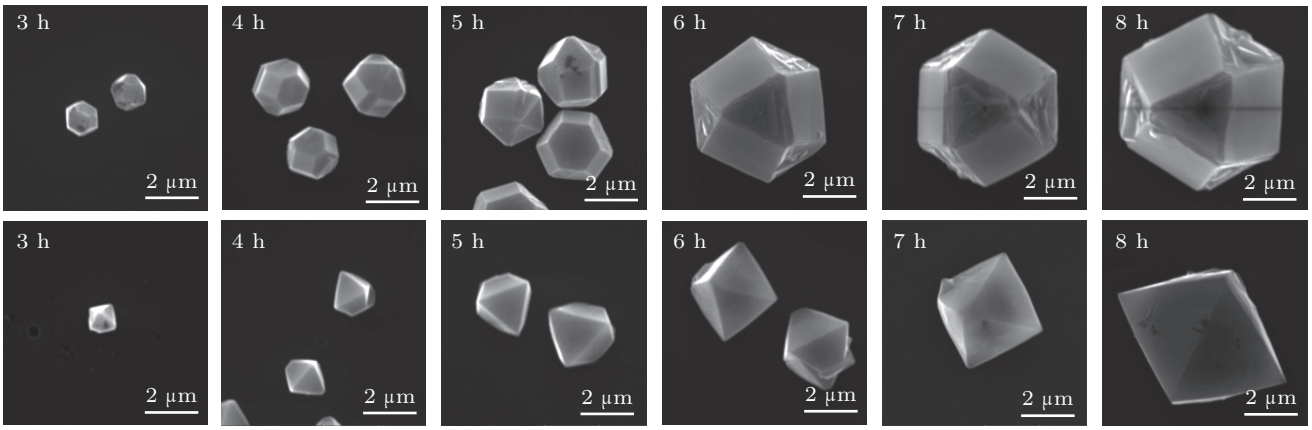


Fig. 3. SEM images of isolated diamond particles grown under 2.5 kPa (upper) and 3.5 kPa (down) for 3–8 h, respectively.

Typical room temperature normalized PL spectra of the isolated diamond particles with different growth times are shown in Fig. 4(a). The SiV PL normalized intensity (see Fig. 2) of diamond particles grown under 3.5 kPa is much stronger than those grown under 2.5 kPa, except the situation of growth time of 3 h. Considering the effect of crystal size on the fluorescence intensity, the variations in the normalized intensity and FWHM values of SiV peak as a function of diamond crystal size are shown in Figs. 4(b) and 4(c), respectively. When the growth pressure is 2.5 kPa, the normalized intensity of SiV PL reaches the maximum with the crystal size of ~ 2 μm, while it gradually decreases with the increase of growth time, even though the crystal size increases. For the growth pressure of 3.5 kPa, the normalized intensity of SiV PL increases dramatically to more than 20 when the crystal size increases to approximately 2 μm, and then it further increases to more than 30 when the crystal size increases to more than 3 μm. In Fig. 4(c), for the samples grown under 2.5 kPa, the values of FWHM vary with the growth time from 6.0 to 6.9 nm. In the case of 3.5 kPa, the range of FWHM values is from 5.0 to 5.5 nm. It is also found that the isolated diamond particles grown under these two growth pressures have similar sizes, as shown by the diagonal filled squares. In each group, the diamond grown under 3.5 kPa shows stronger and narrower SiV PL peak, indicating that the crystal planes play more significant roles than the grain size in the normalized intensity and bandwidth of SiV PL. These results also suggest that appropriate growth condition enables {111}-faceted diamonds to maintain strong SiV emission at different crystal sizes.

Figure 5(a) shows the Raman spectra of these samples. In the case of 2.5 kPa, when the growth time is less than 5 h, the Raman spectra only show a sharp diamond peak. Further increasing the growth time, the diamond peak becomes broad and the non-diamond carbon between 1400 and 1600 cm^{-1} appears, indicating the quality deterioration of diamond crystal. The SEM graphs in Fig. 3 confirm that {111} planes become rough due to the faster growth rate for ⟨111⟩ directions when the growth time is longer than 5 h. For the diamond particles grown under 3.5 kPa, the narrower diamond peaks exist in these samples. When the growth time is more than 6 h, the non-diamond carbon signal also appears, but is weaker than that grown under 2.5 kPa. Correspondingly, the SEM images show that the {111} planes remain smooth, even though the growth time increases.

The detailed changes of FWHM and diamond position values are shown in Figs. 5(b) and 5(c). It is observed that the FWHM values for both series of the samples show a non-linear change with increasing crystal size. In the case of 2.5 kPa, the FWHM values of the diamond peak vary from 7.4 cm^{-1} to 12 cm^{-1} with increasing growth time. For the diamond particles grown under 3.5 kPa, the FWHM value of the diamond peak fluctuates in a smaller range from 6 cm^{-1} to 9.7 cm^{-1}. This suggests smaller FWHM and higher crystal quality of diamond particles grown under 3.5 kPa. Also, their diamond positions vary in the range from 1333.3 to 1334.2 cm^{-1} for the particles grown under 2.5 kPa, and 1332.5 to 1333.5 cm^{-1} for those particles grown under 3.5 kPa, respectively. This indicates that the diamond position of the particles grown under 3.5 kPa is much closer to that of strain-free diamond with the value of 1332 cm^{-1}. These results indicate that the diamond particles consisting of {111} planes maintain a higher

crystal quality and less lattice stress even if the crystal size changes, which is beneficial for the improvement of SiV PL performance.

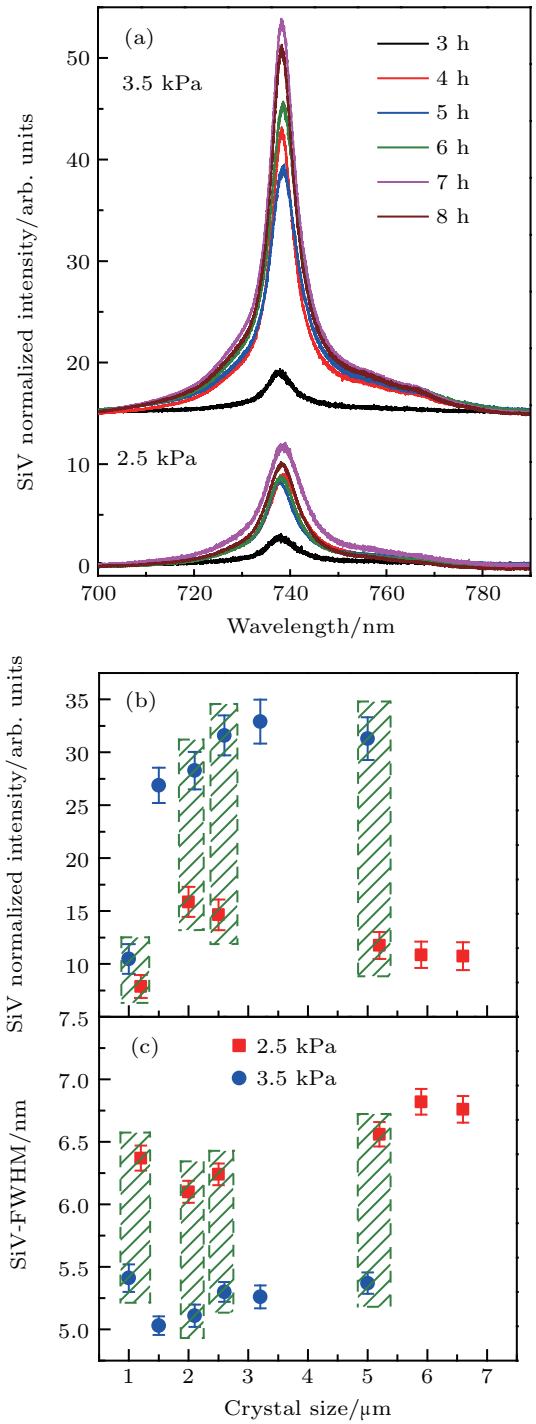


Fig. 4. (a) Typical PL spectra of samples grown under 2.5 and 3.5 kPa for 3–8 h (one of the diamond particles for each growth time). The variation of (b) the normalized intensity and (c) FWHM values of SiV photoluminescent peak with crystal size (averaged over 5 diamond particles for each growth time).

The above room-temperature PL and Raman single-point tests reveal the microstructure and SiV PL performance of diamond particles with different shapes, while the detection area is mainly focused on the near-surface of the particles. Here, we perform the depth profiles of Raman and PL spectroscopy on the samples grown under 2.5 and 3.5 kPa for 4 and 6 h, respectively, to understand the dependence of structure and PL on the depth of the diamond particles. Figure 6(a) is the

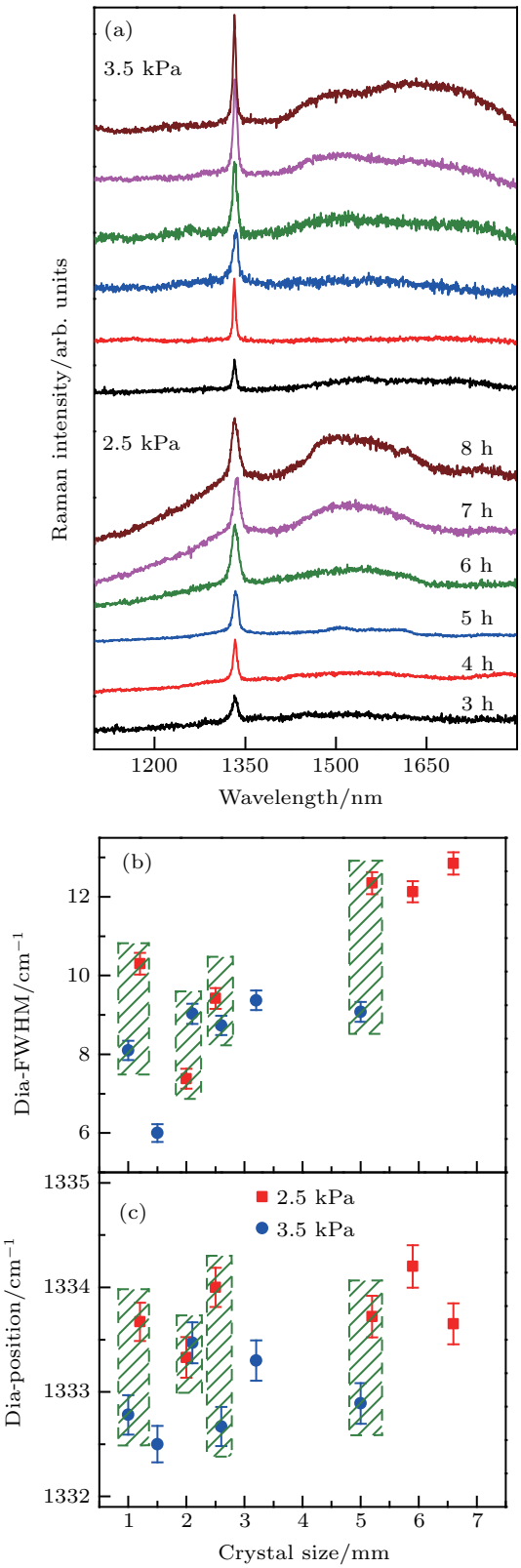


Fig. 5. (a) Typical visible Raman spectra of samples grown under 2.5 and 3.5 kPa for 3–8 h (one of the diamond particles for each growth time). The variation of (b) FWHM and (c) position of diamond peak with crystal size (averaged over 5 diamond particles for each growth time).

schematic illustration of Raman and PL depth profiles tests. Figure 6(b) shows the Raman depth profiles of one of the diamond particles grown under 2.5 kPa for 4 h. From the diamond surface to the substrate, the signals of the diamond peak become weaker and weaker. It is found that the ratios of Si peak to diamond peak ($I_{Si}/I_{diamond}$) vary slightly over a range of depths from the diamond particle surface to the interior, but it increases appreciably at a certain depth, as shown by the inset of Fig. 6(b). The depth ranges at which $I_{Si}/I_{diamond}$ values increase significantly coincide with the size of diamond particles in each group, indicating that the laser focuses have moved to the Si substrate. That is to say, although the laser has some energy loss when it penetrates the diamond particle, it can still collect the information of each depth areas effectively. The PL depth profiles are shown in Fig. 6(c), displaying that the signal of the SiV becomes weaker with increasing depth.

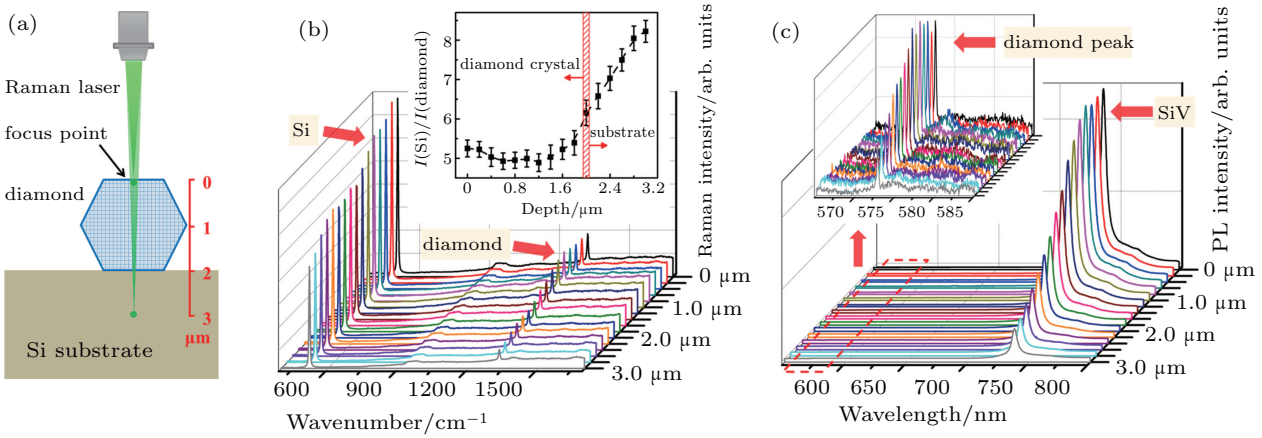


Fig. 6. (a) Schematic illustration of Raman and PL depth profiles tests. (b) The depth profiles of Raman spectra of diamond particles in sample 2.5 kPa-4 h. The inset shows the ratios of the intensity of Si and diamond peak ($I_{Si}/I_{diamond}$) in Raman spectra. (c) The depth profiles of PL spectra of diamond particles in sample 2.5 kPa-4 h. The inset shows the enlarged view of the red dotted box area in the PL spectra, which is responsible for the diamond Raman peak.

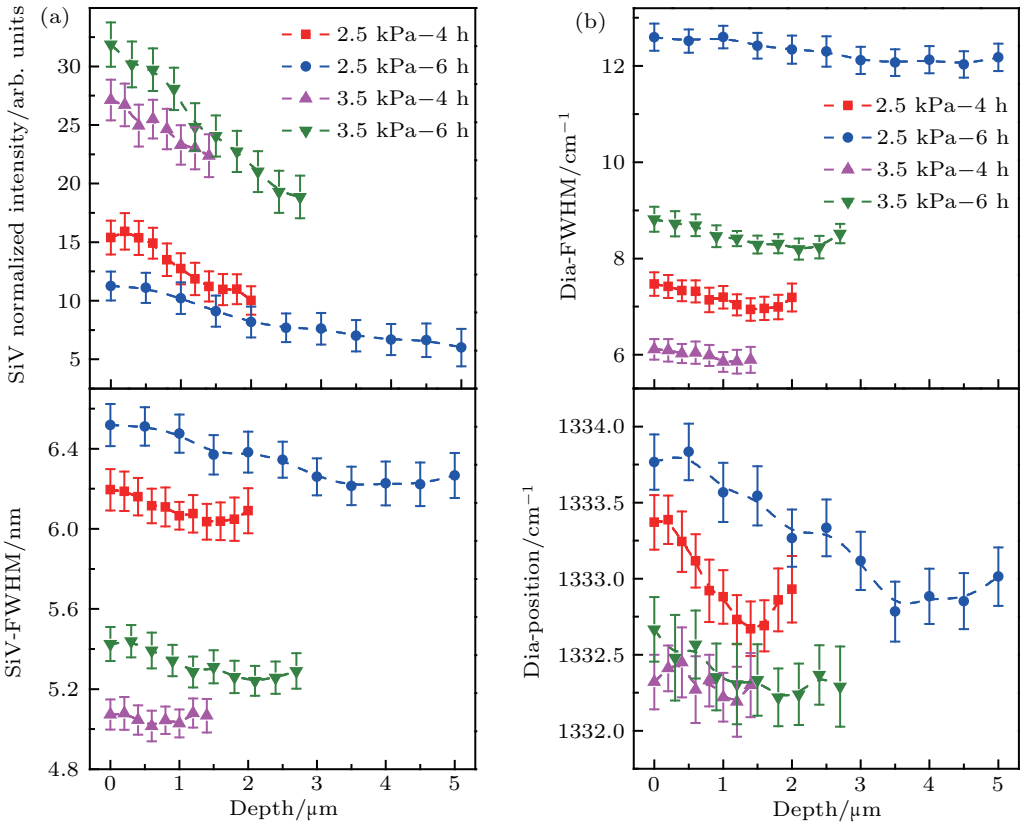


Fig. 7. (a) The depth profiles of normalized intensity and FWHM of SiV peak in the range of crystal size, and (b) the FWHM and position of diamond peak in the range of crystal size for the samples, which were fabricated under 2.5 and 3.5 kPa for 4 and 6 h (averaged over 5 crystals for each selected groups).

Figure 7(a) shows the normalized intensity and FWHM values of SiV PL peaks in the crystal size range for each selected sample. From the upper surface to the near substrate region of the particles, the normalized intensity of SiV PL gradually decreases. This implies that the SiV color center is more easily formed in the near-surface region of the isolated diamond particles. It is also noted that the decreasing amplitude of SiV normalized intensity is more significant for the bigger diamond particles. For the samples grown for 4 h under two selected growth pressures, the reduction of SiV normalized intensity values is less than 30%. For the diamonds grown under 2.5 kPa for 6 h, the crystal sizes are approximately 5 μm, and the reduction of SiV normalized intensity value is 43%. As for the FWHM values of SiV peaks, as shown in Fig. 7(a), they decrease slightly in the near substrate region compared to the near-surface areas, except for the sample grown under 3.5 kPa for 4 h. These results suggest that the bigger the diamond particles, the greater the difference of SiV properties between the near-surface areas and the inner of the diamond.

The microstructure evolution at different depths inside the diamond particle is studied by the variation of the FWHM value and position of the diamond peak in Raman spectra. Figure 7(b) shows that with the change of depth, the variation of the FWHM values of diamond peaks is very small, indicating the crystalline perfection is almost identical in each region of the diamond particle. As for the diamond peak position, it downshifts significantly as the depth increases for the samples grown under 2.5 kPa, while it only has slight fluctuations for the samples grown at 3.5 kPa. It indicates that the samples grown under 3.5 kPa have a small difference in lattice stress between the crystal surface and the interior area. These results also imply that the difference of lattice stress in the diamond particles is more obvious if the growth rate is faster.

Combining the above results of Raman and PL depth profiles tests, we reveal the relationship between SiV PL and the microstructure of diamond particles, as shown in Fig. 8. In the growth process of diamond particles, new atoms including carbon atoms and other small amounts of impurities are continuously bonded in the near-surface areas, as well as the migration of vacancies. Therefore, these regions have poor crystal quality and large lattice stress. In this case, the SiV centers are easy to form. It is noted that because of the complicated stress environment, the FWHM of SiV PL peak is broad. With diamond growth, the near-surface area becomes the inner area and its crystal structure is constantly improved. Some of the SiV centers are not stable due to the movement of the vacancies. Therefore, the SiV normalized intensity will decrease, while the FWHM of the SiV PL peak is narrowed due to the smaller stress. Especially, if the crystal growth rate is very fast, the difference in lattice stress between the surface and the interior will be greater. Our results reveal the relationship between SiV PL properties and the microstructure of both surface and inner areas of the isolated diamond particles.

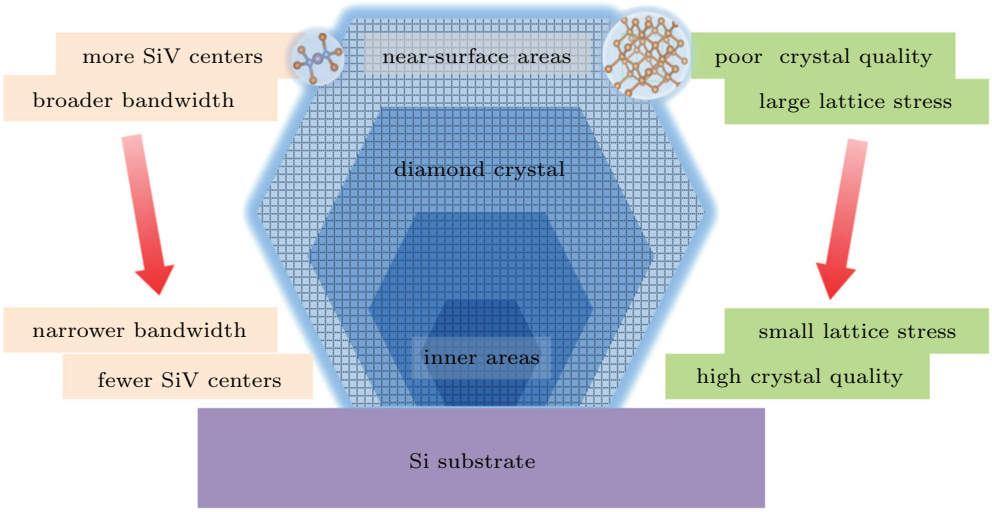


Fig. 8. Schematic illustration of the relationship between SiV PL and microstructure of diamond crystals.

4. Conclusion

In summary, we have fabricated the isolated SiV fluorescent diamond particles with specific crystallographic planes by HFCVD. A non-seeding process is performed, avoiding the effects of nano-diamond seeds on the structure and shape of diamond particles. By adjusting the growth pressure, the diamond particles exhibit the distinct smooth single crystal faceting with different orientations. Under the growth pressure of 2.5 kPa, the diamond particles consist of {100} and {111} planes. With the growth pressure increasing to 3.5 kPa, the diamond particles only consist of {111} planes, which have better crystal quality, stronger intensity, and narrower linewidth of SiV PL. The Raman depth profiles show that compared to the near Si substrate regions, the near-surface areas of the di-

amond particles have poorer crystal quality and greater lattice stress, which give more chances for SiV centers to form in the crystals near-surface areas. The faster the diamond growth rate, the more pronounced difference in the lattice stress between the crystal surface and the interior area. Our study provides a feasible way to prepare diamond particles with specific morphology and stronger SiV PL.

References

[1] Arnault J C 2017 *Nanodiamonds: Advanced Material Analysis, Properties and Applications* (Netherlands: Elsevier) pp. 365–476

[2] Xu H, Ye H T, Coathup D, Mitrovic I Z, Weerakkody A D and Hu X J 2017 *Appl. Phys. Lett.* **110** 033102

[3] Jiang M Y, Yu H, Li X, Lu S H and Hu X J 2017 *Electrochim. Acta* **258** 61

[4] Aharonovich I, Greentree A D and Prawer S 2011 *Nat. Photon.* **5** 397

[5] Pezzagna S, Rogalla D, Wildanger D, Meijer J and Zaitsev A 2011 *New J. Phys.* **13** 035024

[6] Goss J P, Jones R, Breuer S J, Briddon P R and Oberg S 1996 *Phys. Rev. Lett.* **77** 3041

[7] Muller T, Hepp C, Pingault B, Neu E, Gsell S and Schreck M 2014 *Nat. Commun.* **5** 3328

[8] Merson T D, Castelletto S, Aharonovich I, Turbic A, Kilpatrick T J and Turnley A M 2013 *Opt. Lett.* **38** 4170

[9] Vlasov I I, Barnard A S, Ralchenko V G, Lebedev O I, Kanzyuba M V and Saveliev A V 2009 *Adv. Mater.* **21** 808

[10] Rogers L J, Jahnke K D, Doherty M W, Dietrich A, McGuinness L P, Muller C, Teraji T, Sumiya H, Isoya J, Manson N B and Jelezko1 F 2014 *Phys. Rev. B* **89** 235101

[11] Hepp C, Muller T, Waselowski V, Becker J N, Pingault B, Sternschulte H, Steinmüller-Nethl D, Gali A, Maze J R, Atatüre M and Becher C 2014 *Phys. Rev. Lett.* **112** 036405

[12] Sedov V S, Khomich A A, Ralchenko V G, Martyanov A K, Savin S S, Poklonskaya O N and Trofimov N S 2015 *J. Coat. Sci. Technol.* **2** 38

[13] Sun B, Zhang X and Lin Z 1993 *Phys. Rev. B* **47** 9816

[14] Yang S, He Z, Li Q, Zhu D and Gong J 2008 *Diam. Relat. Mat.* **17** 2075

[15] Zhang Y and Chen G 1995 *J. Vac. Sci. Technol. A-Vac. Surf. Films.* **13** 183

[16] Yu Z and Flodstrom A 1997 *Diam. Relat. Mat.* **6** 81

[17] Zhang T, Liu X, Sun F H and Zhang Z M 2015 *J. Cryst. Growth.* **426** 15

[18] Zhang T, Wang X C, Shen B, Sun F H and Zhang Z M 2013 *J. Cryst. Growth.* **372** 49

[19] Stacey A, Aharonovich I, Prawer S and Butler J E 2009 *Diam. Relat. Mater.* **18** 51

[20] Tzeng Y K, Zhang J L, Lu H, Ishiwata H, Dahl J, Carlson R M K, Yan H, Schreiner P R, Vuc?ković J, Shen Z X, Melosh N and Chu S 2017 *Nano. Lett.* **17** 1489

[21] Singh S and Catledge S A 2013 *J. Appl. Phys.* **113** 044701

[22] Zhang H, Aharonovich I, Glenn D R, Schalek R, Magyar A P, Lichtman J W, Hu E L and Walsworth R L 2014 *Small* **10** 1908

[23] Mei Y S, Fan D, Lu S H, Shen Y G and Hu X J 2016 *J. Appl. Phys.* **120** 225107

[24] Hu X J, Chen C K and Lu S H 2016 *Carbon* **98** 671

[25] Petráková V, Taylor A, Kratochvílová I, Fendrych F, Vacik J and Kucka J 2012 *Adv. Funct. Mater.* **22** 812

[26] Galář P, Dzurňák B, Varga M, Marton M, Kromka A and Maly P 2014 *Opt. Mater.* **4** 624